Journal of Experimental Botany, Vol. 60, No. 15, pp. 4221–4234, 2009
doi:10.1093/jxb/erp263 Advance Access publication 28 August, 2009
This paper is available online free of all access charges (see http://jxb.oxfordjournals.org/open_access.html for further details)

Journal of Experimental Botany
www.jxb.oxfordjournals.org

RESEARCH PAPER

Protein targets of tyrosine nitration in sunflower (*Helianthus annuus* L.) hypocotyls

Mounira Chaki[1], Raquel Valderrama[1], Ana M. Fernández-Ocaña[1], Alfonso Carreras[1], Javier López-Jaramillo[3], Francisco Luque[1], José M. Palma[2], José R. Pedrajas[1], Juan C. Begara-Morales[1], Beatriz Sánchez-Calvo[1], María V. Gómez-Rodríguez[1], Francisco J. Corpas[2,*] and Juan B. Barroso[1]

[1] Grupo de Señalización Molecular y Sistemas Antioxidantes en Plantas, Unidad Asociada al CSIC (EEZ), Departamento de Bioquímica y Biología Molecular, Universidad de Jaén, Spain
[2] Departamento de Bioquímica, Biología Celular y Molecular de Plantas, Estación Experimental del Zaidín, CSIC, Apartado 419, E-18080 Granada, Spain
[3] Instituto de Biotecnología, Universidad de Granada, Spain

Received 28 May 2009; Revised 31 July 2009; Accepted 4 August 2009

Abstract

Tyrosine nitration is recognized as an important post-translational protein modification in animal cells that can be used as an indicator of a nitrosative process. However, in plant systems, there is scant information on proteins that undergo this process. In sunflower hypocotyls, the content of tyrosine nitration (NO_2-Tyr) and the identification of nitrated proteins were studied by high-performance liquid chromatography with tandem mass spectrometry (LC-MS/MS) and proteomic approaches, respectively. In addition, the cell localization of nitrotyrosine proteins and peroxynitrite were analysed by confocal laser-scanning microscopy (CLSM) using antibodies against 3-nitrotyrosine and 3′-(*p*-aminophenyl) fluorescein (APF) as the fluorescent probe, in that order. The concentration of Tyr and NO_2-Tyr in hypocotyls was 0.56 μmol mg^{-1} protein and 0.19 pmol mg^{-1} protein, respectively. By proteomic analysis, a total of 21 nitrotyrosine-immunopositive proteins were identified. These targets include proteins involved in photosynthesis, and in antioxidant, ATP, carbohydrate, and nitrogen metabolism. Among the proteins identified, *S*-adenosyl homocysteine hydrolase (SAHH) was selected as a model to evaluate the effect of nitration on SAHH activity using SIN-1 (a peroxynitrite donor) as the nitrating agent. When the hypocotyl extracts were exposed to 0.5 mM, 1 mM, and 5 mM SIN-1, the SAHH activity was inhibited by some 49%, 89%, and 94%, respectively. *In silico* analysis of the barley SAHH sequence, characterized Tyr448 as the most likely potential target for nitration. In summary, the present data are the first in plants concerning the content of nitrotyrosine and the identification of candidates of protein nitration. Taken together, the results suggest that Tyr nitration occurs in plant tissues under physiological conditions that could constitute an important process of protein regulation in such a way that, when it is overproduced in adverse circumstances, it can be used as a marker of nitrosative stress.

Key words: Nitric oxide, nitroproteomics, nitrotyrosine, peroxynitrite, protein tyrosine nitration, reactive nitrogen species.

Introduction

Protein tyrosine nitration is a nitric-oxide-mediated post-translational modification that has been reported mainly in animal cells (Alvarez and Radi, 2003; Ischiropoulos, 2003, 2009), although there are some reports in yeasts (Buchczyk *et al.*, 2000). This covalent alteration is the result of the addition of a nitro ($-NO_2$) group to one of the two equivalent ortho carbons of the aromatic ring of tyrosine residues (Gow *et al.*, 2004; Radi, 2004). So far, there are several mechanisms that are known to mediate protein tyrosine nitration *in vivo* involving either peroxynitrite or nitrite/H_2O_2/haemperoxidase or transition metals (Radi, 2004). This process in proteins may exert different effects,

* To whom correspondence should be addressed: javier.corpas@eez.csic.es

such as loss of protein function, gain of function, or no change in function (Souza *et al.*, 2008). However, the most frequent effect observed for the nitration of tyrosine has been the inactivation of several enzymes that contain critical and susceptible tyrosine residues. Some examples of nitrated enzymes include manganese superoxide dismutase, nitric oxide synthase 2, cytochrome P450, pyruvate kinase, aldolase A, glutathione reductase, and glutamine synthase among others (Wong and van der Vliet, 2002; Schopfer *et al.*, 2003; Peluffo and Radi, 2007; Souza *et al.*, 2008). However, there are other cases where tyrosine nitration caused activation, for example glutathione *S*-transferase (Ji *et al.*, 2006). Moreover, this post-translational modification, apparently involved in cell signalling and cytoskeletal organization, is considered a potential marker of nitrosative stress in some pathologies such as cardiovascular disease (Turko and Murad, 2002; Peluffo and Radi, 2007; Rubbo and Radi, 2008). By contrast, in plant systems, information on this process is scarce (Corpas *et al.*, 2007*a*, *b*, 2008*a*, *b*, 2009), the information available so far being related to the induction of this process under certain stress conditions (Wilhelmova *et al.*, 2006; Valderrama *et al.*, 2007; Corpas *et al.*, 2008*a*, *b*; Chaki *et al.*, 2009). However, there is no information available on the identity of nitrated proteins in plants.

In the present work, by using a combination of analytical, immunological, and proteomic approaches, the content of nitrotyrosine and the identity of potential protein targets for nitration have been determined for the first time in plant tissues. In addition, it is demonstrated, by *in vitro* analyses, that the tyrosine nitration of *S*-adenosyl-homocysteine hydrolase (SAHH) inhibited its activity. An *in silico* analysis revealed that Tyr448 from barley SAHH could be the potential nitration target.

Materials and methods

Sunflower genotypes and growth conditions

Sunflower (*Helianthus annuus* L. lines X55) seeds were obtained from Koipesol Seeds SA (Seville, Spain). Seedlings were sown in wet vermiculite, and grown under optimum conditions for 9 d, with 16/8 h light/dark at 20 °C.

Crude extract of sunflower hypocotyls

Hypocotyls were ground in liquid nitrogen using a mortar and pestle. The resulting coarse powder was transferred into 1/2 (w/v) extraction medium of 0.1 M TRIS-HCl, buffer, pH 7.6, containing 5% (w/v) sucrose, 7% (w/v) PVPP, 0.05% (v/v) Triton X-100, 0.1 mM EDTA, 15 mM DTT, 1 mM PMSF, and a commercial cocktail of protease inhibitors (AEBSF, 1,10-phenanthroline, pepstatin A, leupeptin, bestatin, and E-64) (Sigma, St Louis, MO, USA). The crude extracts were then filtered through one layer of Miracloth (Calbiochem, San Diego, CA, USA), centrifuged at 3000 *g* for 6 min (4 °C), and the supernatants were used for immunoblot analyses.

Determination of nitrotyrosine and tyrosine by high-performance liquid chromatography with tandem mass spectrometry (LC-MS/MS)

Sunflower hypocotyls were ground using a mortar and pestle in liquid nitrogen, and were suspended into 1/2 (w/v) digestion buffer (50 mM sodium acetate, pH 6.5) according to Hensley *et al.* (1998). Homogenates were filtered through one layer of Miracloth (Calbiochem), centrifuged at 3000 *g* for 5 min and the supernatant proteins were precipitated by the addition of 10% trichloroacetic acid (TCA). After incubation at 4 °C for 20 min the samples were centrifuged at 14 000 *g* for 10 min. Protein pellets were washed twice with acetone at –20 °C, air-dried, and resuspended in 1 ml of digestion buffer containing 4 mg of pronase (Calbiochem), and incubated at 50 °C for 30 h with gentle stirring. The digested samples were treated with 10% TCA at 4 °C for 20 min followed by centrifugation at 14 000 *g* for 10 min. The supernatants were passed through 0.45 µm PVDF filter. Samples were analysed by high-performance liquid chromatography with tandem mass spectrometry (LC-MS/MS) for tyrosine (Tyr) and 3-nitrotyrosine (NO_2-Tyr) by the method of Ishi *et al.* (2006). Mass-spectrometric measurements were carried out using a Bruker Daltonics Esquire-LC ion trap MS with an electrospray ionization interface at atmospheric pressure (Bruker Daltonics, Bremen, Germany) coupled to an Agilent 1100 LC system (Agilent Technologies) and equipped with a Waters Spherisorb® 3×125 mm C18 column with 5 µm particle size, (Waters SAS, France). The mobile phase consisted of 0.1% formic acid in water (solvent A) and acetonitrile with 0.1% formic acid (solvent B) at a constant flow rate of 0.45 ml min^{-1}. The column was equilibrated with a mixture of 97% solvent A and 3% solvent B. Injection volumes of 20 µl of the samples were used and the compounds were eluted from the column using a continuous gradient beginning with 3% solvent B in solvent A and programmed to 70% B in 9 min, with the column being flushed for another 3 min at 70% B prior to returning to 3% B in 3 min and holding for 5 min before beginning the next injection in the sequence. The column effluent was directed into the electrospray source. Under these conditions, the retention times of tyrosine and nitrotyrosine standards were 5.3 min and 7.0 min, respectively. The optimized working conditions for LC/MS using electrospray ionization with positive ion polarity were as follows: trap drive 34.0, capillary exit 100 V, nebulizer 40 psi, dry gas 9.0 l min^{-1}, dry temperature 350 °C, HV capillary 4000 V, HV endplate offset – 500 V, spectral averages 10, and the fragmentation amplitude set at 0.8 V for tyrosine and 0.5 V for nitrotyrosine. The precursor ions had a mass of 181.8 *m/z* and 226.7 *m/z* and the selected product ions had a mass of 135.9 *m/z* and 180.8 *m/z* for tyrosine and nitrotyrosine, respectively. Samples were diluted at the ratio of 1 to 10 000 before assay. The LC-ESI-MS/MS system was controlled using an Agilent Chemstation LC 3D and Bruker Daltonics Esquire 5.2 DataAnalysis software was used for the data analysis.

Calibration curves were prepared with tyrosine and nitrotyrosine standards of 0.1–1000 μM and 0.5–1000 nM, respectively.

Electrophoretic methods and Western blot analyses

Polypeptides were separated by 12% SDS–PAGE, and proteins were transferred to polyvinylidene fluoride (PVDF) membranes (Immobilon P, Millipore Corp., Bedford, MA, USA) using a Semi-Dry Transfer System (Bio-Rad), as described by Corpas *et al.* (1998). For immunodetection, a rabbit polyclonal antibody against 3-nitrotyrosine (NO_2-Tyr) (Uttenthal *et al.*, 1998) diluted 1:5000 was used, and immunoreactive bands were detected with a photographic film (Hyperfilm; Amersham Pharmacia Biotech) with an enhanced chemiluminescence kit (ECL-PLUS, Amersham Pharmacia Biotech).

Protein concentration was determined with the Bio-Rad Protein Assay (Hercules, CA, USA), using bovine serum albumin as a standard.

Nitrotyrosine immunohistochemistry by confocal laser-scanning microscopy (CLSM)

Sunflower hypocotyls were cut into 4–5 mm pieces and fixed in 4% (w/v) *p*-formaldehyde prepared in 0.1 M phosphate buffer (PB), pH 7.4, for 3 h at room temperature. Then, they were cryoprotected by immersion in 30% (w/v) sucrose in PB overnight at 4 °C. Serial sections, 60 μm thick, were made by means of a cryostat (2800 Frigocut E, Reichert-Jung, Vienna, Austria).

Immunohistochemistry was performed by confocal analysis of immunofluorescence-stained sections, as described by Valderrama *et al.* (2006). Free-floating sections were incubated overnight at room temperature with a rabbit polyclonal antibody against 3-nitrotyrosine (Uttenthal *et al.*, 1998) diluted 1:300 in 5 mM TRIS-HCl buffer, pH 7.2, 0.9% (w/v) NaCl, containing 0.05% (w/v) sodium azide, 0.1% (w/v) bovine serum albumin and 0.1% (v/v) Triton X-100 (TBSA-BSAT). After several washes with TBSA-BSAT, the sections were incubated with biotinylated goat anti-rabbit IgG (Pierce), diluted 1:1000 in TBSA-BSAT, for 1 h at room temperature. Sections were washed again and incubated with Cy2-streptavidin (Amersham), diluted 1:1000 in TBS-BSAT, for 1.5 h at room temperature, this and the following steps being performed in the dark. After several washes, sections were then mounted in PBS:glycerol 1:1 v/v. Hypocotyl cross-sections were examined with a confocal laser-scanning microscope (Leica TCS SL) using standard filters for Cy2- streptavidin (excitation 492 nm; emission, 510 nm). Controls for background staining were performed by replacing the primary antibody with an equivalent concentration of either of the incubation buffer or rabbit pre-immune serum.

Detection of peroxynitrite by confocal laser-scanning microscopy (CLSM)

Peroxynitrite ($ONOO^-$) was detected with 10 μM 3′-(*p*-aminophenyl) fluorescein (APF, Invitrogen) prepared in 10 mM TRIS-HCl (pH 7.4). Transversal hypocotyl cross-sections were incubated at 25 °C for 1 h, in darkness. After incubation, samples were washed twice in the same buffer for 15 min each. Hypocotyl sections were then embedded in a mixture of 15% acrylamide-bisacrylamide stock solution as described elsewhere (Corpas *et al.*, 2006), and 80–100 mm thick sections were cut under 10 mM phosphate-buffered saline (PBS). Sections were then soaked in glycerol:PBS (containing azide) (1:1 v/v) and mounted in the same medium for examination with a CLSM system (Leica TCS SL), using standard filters and collection modalities for APF green fluorescence (excitation 495 nm; emission 515 nm).

As a control, sections were preincubated for 2 h at 25 °C with 20 μM Ebselen (a peroxynitrite scavenger) (Daiber *et al.*, 2000; Chander *et al.*, 2004).

Protein precipitation

Hypocotyls (168 g) of 1000 sunflower seedlings were processed for crude extracts as mentioned above. For protein precipitation, 3 vols of 100% acetone at –20 °C were added to the supernatants with continuous stirring for 60 min (70% final concentration, v/v) and the mixture was centrifuged at 16 000 *g* for 15 min. The precipitate, which contained most of the proteins, was taken up into 150 ml of 50 mM HEPES pH 7.6, 50 mM NaCl (buffer A) and centrifuged again at 16 000 *g* for 15 min. The supernatants were passed through Sephadex G-25 gel-filtration columns (NAP-10 from Amersham) which were equilibrated with buffer A.

Two-dimensional (2D) gel electrophoresis and immunoblot analysis

Proteins were separated by two-dimensional gel electrophoresis. Isoelectric focusing was carried out with precast IPG-gels pH 3–10. Each gel was loaded with 100 μg of proteins. Second-dimensional separation was performed by Glycine-SDS-PAGE according to Laemmli (1970). Gels were SYPRO Ruby stained, scanned, and analysed with Bio-Rad PD Quest software. Western blot of 2D gels was performed as described above.

In situ *digestion of 2D spots and protein identification by MALDI TOF-TOF analysis*

Identified spots in the gel were automatically recovered using Investigator ProPic Protein Picking Workstation (Genomic Solutions). Then, they were digested with trypsin using an Investigator™ ProGest Protein Digestion Station (Genomics Solutions). Briefly the procedure was as follows: spot destaining with 40% acetonitrile/200 mM NH_4HCO_3 for 30 min (twice); washing with 25 mM NH_4HCO_3 for 5 min and further with 25 mM NH_4HCO_3/50% acetonitrile for 15 min, respectively (twice). Samples were then redehydrated with 100% acetonitrile for 5 min and dried. The samples were hydrated with 10 μl trypsin in 25 mM NH_4HCO_3 (12.5 ng μl^{-1}) at room temperature for 10 min

and then digested at 37 °C for 12 h. The reaction was stopped by adding 10 µl of 0.5% trifluoroacetic acid (TFA). Peptides were purified using a ProMS station (Genomic Solutions) with a C18 column (ZipTip, Millipore) and eluting with α-cyano-4-hydroxycinnamic acid (3 mg ml^{-1}) in 70% acetonitrile/0.1% TFA in a MALDI plate (1 µl). After crystallization the samples were analysed using a MALDI TOF-TOF Mass Spectrometer in a range mass-to-charge ratio (*m/z*) of 800–4000 Da using a spectrometer 4700 Proteomics Analyser (Applied Biosystems) in automatic mode. Internal calibration of the mass spectrums was performed using the *m/z* of the peptides from porcine trypsin autolysis (mass MH^+=842.509, mass MH^+= 2211.104), given a precision in the *m/z* ratio of 20 ppm. From each sample, the three spectrums with the highest *m/z* ratios were selected. The protein was identified by combining the MS spectrum with the corresponding MS/MS using the MASCOT program from the database of MatrixScience (http://www.matrixscience.com/). The following search parameters were applied, limiting the taxonomic category to green plants: a mass tolerance of 100 ppm and one incomplete cleavage were allowed; complete alkylation of cysteine by carbamidomethylation and partial oxidation of methionine.

Treatment with SIN-1 (peroxynitrite donor) and S-adenosyl homocysteine hydrolase activity assay

The molecule SIN-1 (3-morpholinosydnonimine), being a protein-nitrating compound, has been demonstrated to generate peroxynitrite (Daiber *et al.*, 2004). Thus, hypocotyl samples were passed through Sephadex G-25 gel-filtration columns (NAP-10 from Amersham) equilibrated, and eluted with 100 mM K-phosphate buffer pH 7.2 containing 2 mM potassium cyanide (inhibitor of CuZn-SOD) and 2 mM sodium azide (inhibitors of CuZn-SOD and peroxidases). Aliquots of these samples were incubated at 37 °C for 2 h with increased concentrations (0–5 mM) of SIN-1 (Calbiochem) made up fresh before use. Then, the samples were passed again through a NAP-10 column to avoid any interference of SIN-1 with the activity assay.

S-adenosyl homocysteine hydrolase (EC 3.3.1.1) catalyses the hydrolysis of *S*-adenosylhomocysteine to form adenosine and homocysteine. The activity was assayed according to Kloor *et al.* (2000) with some modifications. The *S*-adenosyl-L-homocysteine (SAH) hydrolysis activity was assayed in a total volume of 1 ml at 37 °C. The reaction mixture contained, at the final concentration of 16 µM SAH (Sigma Chemical Co.), 3 U ml^{-1} adenosine deaminase (Sigma Chemical Co.), 360 mU ml^{-1} nucleoside phosphorylase, 60 mU ml^{-1} xanthine oxidase (Sigma Chemical Co.), and 100 mM potassium phosphate, pH 7.2. The reaction was started by the addition of sunflower samples (10–15 µg of protein). The uric acid formed by the coupled action of SAHH and XOD was measured spectrophotometrically at 292 nm. One unit of activity was defined as the amount of enzyme required to hydrolyse 1.0 nanomoles of *S*-adenosyl-L-homocysteine to adenosine and L-homocysteine min^{-1} at pH 7.2 and 37 °C.

Sequence alignment, modelling and molecular-evolution analysis

Multiple sequence alignments were performed using the ClustalW2 program (http://www.ebi.ac.uk/ Tools/clustalw2/). The tertiary structure of *S*-adenosyl-homocysteine hydrolase was generated by homology modelling at the Swiss Model Server (Arnold *et al.*, 2006) using the coordinates of the *S*-adenoslyl-homocystein hydrolase from *Plasmodium falciparum* (PDB access code 1v8b) as a template. Model quality was evaluated by atomic non-local environment assessment (ANOLEA) (Melo and Feytmans, 1998), three-dimensional profiles (Verify3D) (Eisenberg *et al.*, 1997) and Procheck (Laskowski *et al.*, 1993). The coordinates of the quaternary structure were calculated by the superposition of the model on those of the X-ray structure 1v8b with XtalView (McRee, 1993) and refined with CNS (Brunger *et al.*, 1998) by 50 cycles of rigid body minimization with no experimental energy term. Molecular–evolution studies were carried out at the Evolutionary Trace Server (Mihalek *et al.*, 2004) using a model of the tertiary structure as a template and evolutionary conservation was ranked according to rho parameter that deviates from 1 as variability increases.

Secondary structural analysis was carried by DSSP software (Kabsch and Sander, 1983). Tyrosine phosphorylation predictions were carried out at NetPhos 2.0 Server (Blom *et al.*, 1999).

Results

Hypocotyls from sunflower plants cultivated under optimal conditions were used as the model because, in a previous study, the metabolism of reactive nitrogen species had been characterized (Chaki *et al.*, 2009). To identify and quantify nitrotyrosine (NO_2-Tyr) in hypocotyls, high-performance liquid chromatography with tandem mass spectrometry (LC-MS/MS), that had been used successfully in animal tissues, was adapted (Ishii *et al.*, 2006). Figure 1 shows a typical multiple-reaction monitoring chromatogram and product ion spectra of standards of 1 µM tyrosine (Fig. 1A) and 0.5 nM nitrotyrosine (Fig. 1B). The average retention times of tyrosine (Tyr) and nitrotyrosine (NO_2-Tyr) were 5.3 min and 7.0 min, respectively. Based on this method, Table 1 shows the concentrations of NO_2-Tyr and Tyr mg^{-1} of protein obtained in hypocotyl samples. The ratio of NO_2-Tyr/Tyr was 33.9 µmol mol^{-1}.

On the other hand, the presence of protein targets for tyrosine nitration were studied using a well-characterized antibody against 3-nitrotyrosine (Valderrama *et al.*, 2007; Chaki *et al.*, 2009). Figure 2 shows the immunoblot analysis of the proteins that were apparently affected by tyrosine nitration. A pattern of six immunoreactive bands with molecular masses of 68, 59, 37, 30, 20, and 15 kDa was found, the most abundant being nitrated protein having 68

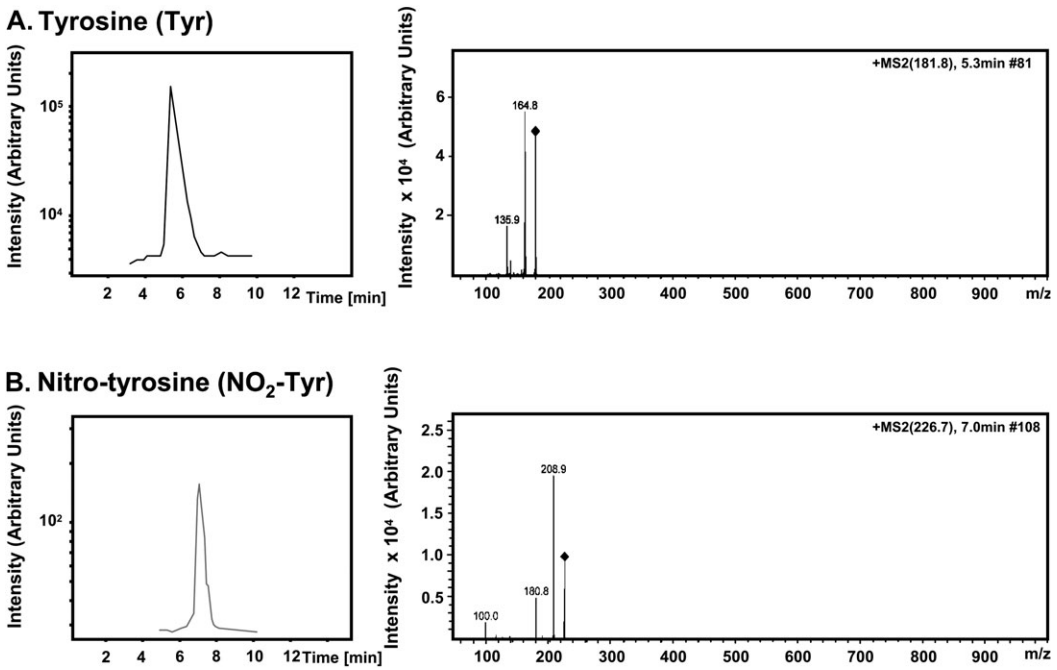

Fig. 1. Multiple-reaction-monitoring chromatograms and product-ion spectra of standards of 1 μM tyrosine (A) and 0.5 nM nitrotyosine (B). The typical standard retention times were 5.3 min and 7.0 min for tyrosine and nitrotyrosine, respectively. The precursor ions had a mass of 181.8 *m/z* and 226.7 *m/z* (filled diamond) and the selected product ions had a mass of 135.9 *m/z* and 180.8 *m/z* for tyrosine and nitrotyrosine, respectively.

Table 1. Concentration of nitrotyrosine (NO_2-Tyr) and tyrosine (Tyr) in sunflower hypocotyls determined by high-performance liquid chromatography with tandem mass spectrometry (LC-MS/MS)

Data are the mean ±SEM of at least three independent experiments.

NO_2-Tyr (pmol mg^{-1} protein)	Tyr (μmol mg^{-1} protein)	NO_2-Tyr/Tyr (μmol mol^{-1})
0.19±0.02	0.56±0.06	33.9±3.2

kDa and 59 kDa subunit sizes. As a positive antibody control, nitrated bovine serum albumin (NO_2-BSA; Sigma, St Louis, MO, USA) was used.

The cell localization of tyrosine nitration of proteins was also analysed in hypocotyl cross-sections by confocal laser-scanning microscopy (CLSM), using the same antibody. The green fluorescence corresponding to the nitrated proteins was observed in vascular tissue, and epidermal and cortex cells (Fig. 3A). When the primary antibody against NO_2-Tyr was substituted by preimmune serum, no immunofluorescence background was detected (Fig. 3B). Peroxynitrite has been shown to mediate protein-tyrosine nitration (Radi, 2004). Therefore, in the study of the possible correlation of nitration and peroxynitrite, this molecule was also detected in hypocotyl sections using the fluorescence probe 3′-(*p*-aminophenyl) fluorescein (APF). Figure 3C shows that peroxynitrite was present mainly in vascular tissue and epidermal cells. When the samples were preincubated with Ebselen (a peroxynitrite scavenger) the green fluorescence was substantially reduced (Fig. 3D). The

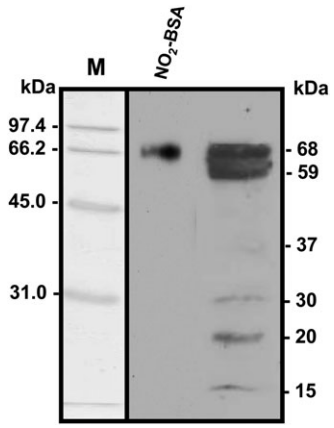

Fig. 2. Detection of tyrosine-nitrated proteins of sunflower hypocotyl crude extracts. Representative immunoblot of hypocotyl crude extracts were incubated with purified IgGs from a rabbit polyclonal 3-nitrotyrosine antibody (dilution 1:5000). Proteins (20 μg) were separated by 10% SDS-PAGE and transferred onto a PVDF membrane. Commercial nitrated bovine serum albumin (NO_2-BSA) (1 μg protein) was used as positive control. M, molecular weight markers.

appearance of the sunflower hypocotyl sections under optical microscopy is shown in Fig. 3E, where the main typical tissues such as epidermis, cortex, vascular tissue (xylem and phloem), and pith are depicted.

To identify the proteins that undergo tyrosine nitration, a proteomic approach was used. Considering that, usually, few proteins seem to be nitrated, enriched crude extracts

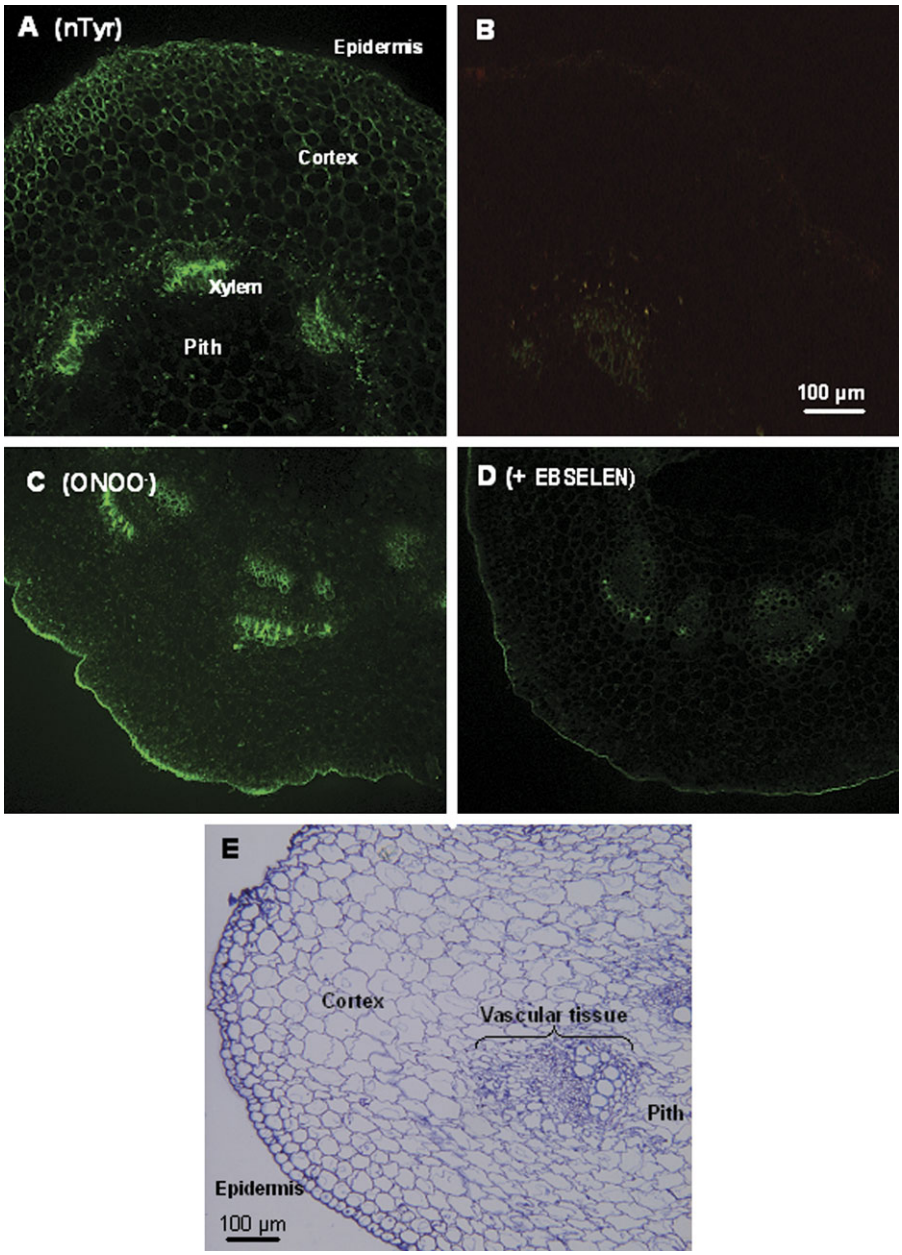

Fig. 3. Representative images illustrating the confocal laser-scanning microscopy detection of protein 3-nitrotyrosine (NO_2-Tyr) (A) and peroxynitrite (C) in cross-sections of sunflower hypocotyls. Protein 3-nitrotyrosine (NO_2-Tyr) was detected using a specific antibody at a dilution of 1:300 as described in the Materials and methods. The bright-green fluorescence corresponds to the detection of NO_2-Tyr. As a control of immunolocalization, the primary antibody was omitted (B). Peroxynitrite ($ONOO^-$) detection was carried out using 3′-(*p*-aminophenyl) fluorescein (APF) (C). As a control, the sample was preincubated with Ebselen (D). (E) Appearance under the optical microscope of a sunflower hypocotyl section.

were prepared by precipitation with 70% acetone. Figure 4A and B shows the separation of proteins after 2D electrophoresis and its corresponding immunoblot probed with the antibody against NO_2-Tyr, respectively. Thus, a total of 21 immunoreactive spots were detected. These spots were analysed by MALDI-TOF mass spectrometry after trypsin digestion using the MASCOT search engine to analyse MS data to identify proteins from primary-sequence databases (Perkins *et al.*, 1999). The immunoreactive proteins identified are listed in Table 2, the protein-score confidence interval (C.I.) in all cases being higher than 99%, indicating that the proteins were not identified by random matches of peptide-mass data.

To study the significance of tyrosine nitration in enzymatic activity, among the proteins with a CI protein score of 100%, *S*-adenosyl-L-homocysteine hydrolase (SAHH) was selected as a model because, in a previous study, it was also investigated as a potential target of RNS such as *S*-nitrosylation (Lindermayr *et al.*, 2005). For this, hypocotyl samples were incubated with different concentrations of SIN-1, a peroxynitrite-generating system which had been shown to mediate tyrosine nitration (Daiber *et al.*, 2004;

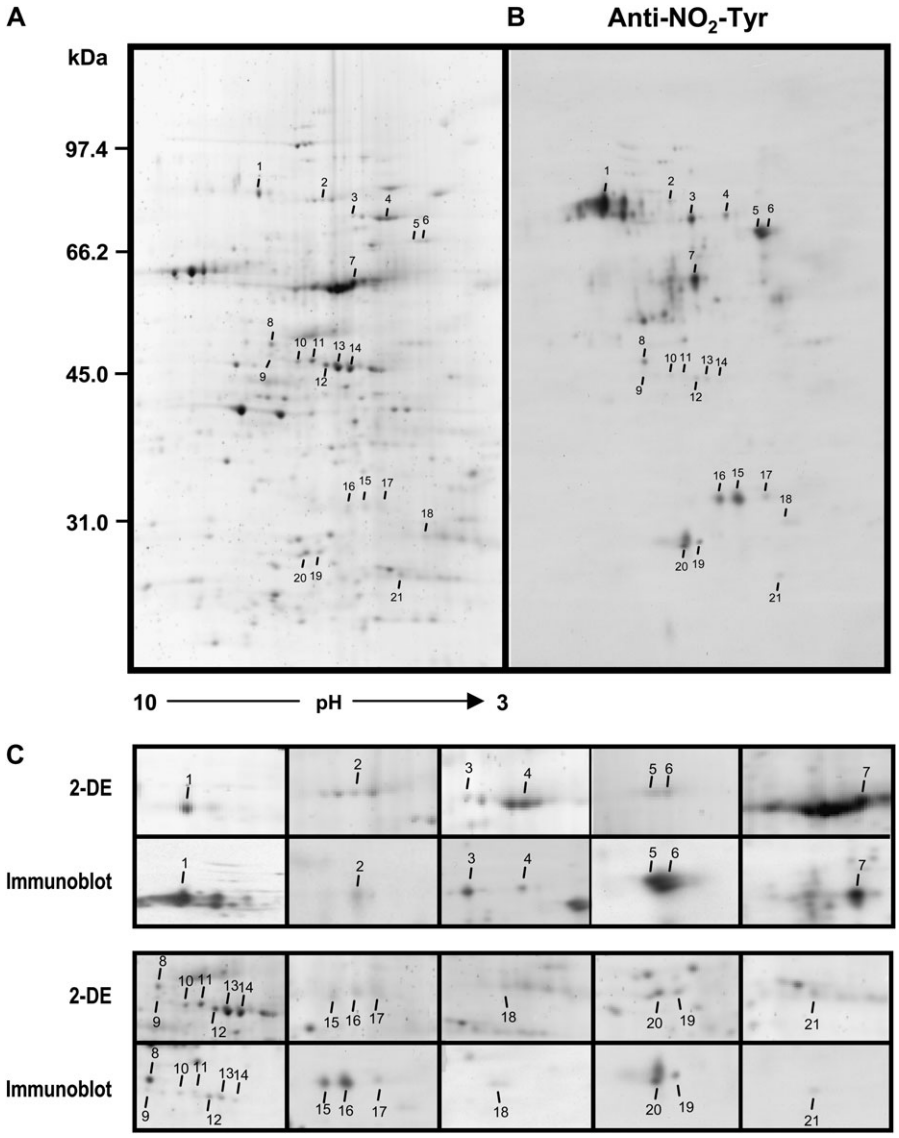

Fig. 4. Detection of nitrated proteins in sunflower hypocotyls by 2-D electrophoresis and immunoblot. (A) Representative 2D electrophoresis (pH 3–10 for the first dimension) of the concentrated hypocotyl extracts stained with Spypro Ruby. Molecular-mass standards are indicated on the left in kDa. (B) The corresponding Western blot of hypocotyl crude extracts probed with a polyclonal antibody against nitrotyrosine (dilution 1:10 000). Approximately 150 μg of proteins were loaded per gel. The arrows indicate all the immunoreactive spots, and the numbers refer to the proteins listed in Table 1. (C) Zoom boxes illustrate details of immunoreactive spots.

Radi, 2004; Larrainzar *et al.*, 2008). Figure 5 depicts the effect of peroxynitrite on SAHH activity in hypocotyl extracts. When the samples were incubated at 37 °C for 2 h with 0.5 mM, 1 mM, and 5 mM of SIN-1, the SAHH activity was inhibited by 49%, 89%, and 94%, respectively.

The full protein sequence of sunflower *S*-adenosyl-L-homocysteine hydrolase (SAHH) is unknown. However, the sequence of its counterparts from *Hordeum vulgare* (Q4LB20), *Triticum aestivum* (P32112), *Oryza sativa* (AAO72664), *Arabidopsis thaliana* (CAB09795), and *Petroselinum crispum* (Q01781) share an overall identity of 83–92% and 100% for the 12 Tyr residues (see Supplementary Fig. S1 at *JXB* online), making it feasible to analyse our results on the basis of these sequences. It has been suggested that both the presence of the nearby amino acids and the solvent exposure of the aromatic ring are predictive factors for the nitration of specific tyrosine *in vivo* (Sacksteder *et al.*, 2006; Abriata *et al.*, 2009). Thus, to gain deeper insight into the potential tyrosine target of nitration the tertiary structure of *Hordeum vulgare*, the SAHH sequence was calculated by homology modelling using as a template the structure of its counterpart from *Plasmodium falciparum* (Tanaka *et al.*, 2004), which shares 58% identity (E-score 2.5698e-165 for the alignment). The refinement converged at –14989.541 KJ mol^{-1} and encompasses the full sequence (450 residues). The analysis of the quality of the model yielded 84.03% of the residues with an average 3D-1D score greater than 0.2 and 86.2% in the most favoured regions in the Ramachandran plot. The few residues in unfavourable non-local atomic interaction energy were located in loop regions. The tertiary-structure model was the input for the evolutionary analysis of the structure. A BLASTP search

Table 2. 3-nitrotyrosine proteins identified from sunflower hypocotyls

Concentrated sunflower hypocotyl extracts were subjected to 2D electrophoresis and immunoblot probed with an antibody against 3-nitrotyrosine. The identified spots were analysed by MALDI-TOF mass spectrometry after trypsin digestion. The MASCOT search engine was used to parse MS data to identify proteins from primary sequence databases. The closer value of Protein Score Confidence Interval (C.I.) to 100% indicates a strong likelihood that the protein is correctly matched. Pep. Count., number of identified peptides. MW, molecular weight. pI, isoelectric point.

Spot no.	Identified protein	Acc. no.	Protein score C.I.%/Pep. Count	MW/pI	Functional grouping
1	Alpha-mannosidase	Q9FFX7	100/6	116918.1/6.0	Mannose metabolic process Carbohydrate metabolism
2	Transketolase precursor	S58083	100/12	75577.1/5.79	Carbohydrate metabolism
3	ATPase-like protein	H85431	99.89/6	69731.6/ 6.99	Energy metabolism. ATP binding. Oxidative phosphorylation
4	Molecular chaperone HSP68	T07024	99.99/11	73317.1/6.37	Protein folding
5	CAD ATPase (AAA1), 35570-33019	B96835	99.918/12	57485.9/6.95	Energy metabolism. ATP binding. Oxidative phosphorylation
6	Ferredoxin-nitrite reductase	*S16603*	*99.59*/12	*67093.2/6.51*	Nitrogen metabolism
7	Glutathione reductase	Q6F4I4	100/14	61175.5/8.75	Antioxidant metabolism
8	Putative serine/threonine-protein kinase	Q84YQ2	99.716/11	53561.8/9.74	Post-translational modifications
9	Alternative oxidase	Q9SC31	99.303/8	40246.2/7.75	Energy metabolism.
10	Putative cytochrome P450	Q9FW84	99.808/11	49131.6/9.64	Biosynthetic reactions of fatty acid conjugates, plant hormones and defensive compounds
11	Putative dehydratase/deaminase	Q8W314_ORYSA	99.966/13	65954.7/5.77	Isoleucine biosynthetic process
12	Ferredoxin-NADP reductase precursor	S04030	99.723/22	40453.7/8.56	Photosynthesis
13	Hypothetical protein	Q75L89	99.72/12	66365.6/5.31	Unknown protein
14	Transposon protein, putative, CACTA, En/Spm sub-class.	Q2QN81	99.609/16	49380.1/6.07	DNA metabolism
15	Acetyl-CoA carboxylase	Q9FEH8	99.407/17	201697.5/6.05	Fat metabolism in higher plants
16	Putative DNA-damage-repair/toleration protein DRT102	Q2PEP7	99.799/14	33287.6/5.22	DNA metabolism
17	*S*-adenosyl-homocysteine hydrolase	Q9SDP1	100/15	34216.2/4.99	Amino-acid biosynthesis
18	14-3-3-like protein	T12951	99.994/5	29043.5/4.65	Regulating cell-signalling
19	20S proteasome subunit C8	G84667	100/9	27644.9/5.93	Proteasome pathway
20	Proteasome endopeptidase complex (EC 3.4.25.1) chain PAA2	T51967	100/6	27446.9/5.75	Proteasome pathway
21	Calmodulin-like protein	Q67TZ4	99.864/8	21417.7/8.68	Calcium binding protein

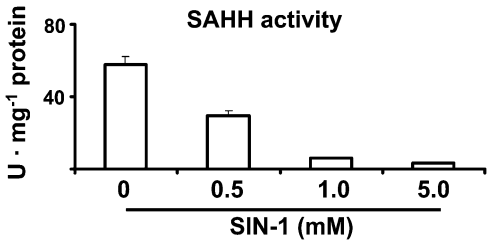

Fig. 5. Effect of SIN-1 ($ONOO^-$ donor) on *S*-adenosyl-L-homocysteine hydrolase (SAHH) activity in sunflower hypocotyl extracts. Samples (see Materials and methods) were incubated at different concentrations of SIN-1 at 37 °C for 2 h.

(Altschul *et al.* 1997) found 500 sequences with *E*-value <*e*-102, and the evolutionary conservation of the different Tyr residues were ranked according to the rho parameter that combines evolutionary and entropy scores (Mihalek *et al.*, 2004). Each tyrosine was further characterized in terms of amino acid content within a nine-residue window of linear sequence around the tyrosine (primary structure), solvent accessible surface area (ASA), secondary structure organization, residues within 5 Å from the atom susceptible of undergoing nitration and phosphorylation susceptibility. The results are summarized in Table 3.

On the other hand, the analysis of the quaternary structure model revealed a relationship between the rho value and the proximity to the NAD-binding site (Fig. 6), where the Tyr residues with smaller rho values are located closer to the cofactor side. A more detailed analysis revealed that the Tyr207 makes a single contact with residues Met268 from the neighbour subunit within 5 Å and that the Tyr residue at position 448 makes a remarkable interaction with NAD.

Discussion

In mammals, tyrosine nitration is being intensively studied because it can be used as a marker of certain pathologies and nitrosative stress (Ischiropoulos, 2003; Tsikas *et al.*, 2005; Rubbo and Radi, 2008). However, new studies are starting to point out the possible implication of tyrosine

Table 3. Characterization of the 12 tyrosine (Y) residues present in SAHH from *Hordeum vulgare* (accession number Q4LB20) in terms of revolutionary conservation (rho score), amino acid content within a nine-residue window of linear sequence around the tyrosine (Primary structure), solvent-accessible surface area (ASA), secondary-structure organization, residues within 5 Å from the two carbons susceptible to nitration (residues from neighbouring subunits are shown in bold) and their potential as target for tyrosine phosphorylation (phosphorylation score)

Rho	Primary structure	ASA (Å^2)	Secondary structure	Residues within 5 Å from the potential nitration target (atom)	Phosphorylation score
1.10	FDNLY^{207}GCRH	19	helix	**Met268**, Phe203 **Met268,** Arg210, Glu269, Leu206	0.387
6.01	SQSDY^{434}ISIP	70	helix	**Lys176, Asn292**	0.985
7.28	KPAAY^{448}RY–	41	loop	NAD, Asp237 **Lys444**, **Tyr450**	0.020
9.13	TLEEY^{82}WWCT	7	helix	Trp83, Asp107, Thr86 Glu77	0.160
10.12	AAYRY^{450}——	8	loop	**Asp259, Cys262**, Lys444, **Ile261, Val198**, Lys406, **Arg449**	0.042
13.06	VVCGY^{235}GDVG	16	loop	Ala266, Val255, Ala243 Lys240, Gln265	0.468
14.35	ASGKY^{397}EKKV	32	loop	Lys396, Leu388, Lys396, Tyr402	0.725
15.14	EKKVY^{402}VLPK	54	beta sheet		0.837
15.47	VKRLY^{179}QMQE	141	helix	Glu183	0.039
21.00	DASKY^{157}RKMK	12	helix	Lys156, Met160, Glu87	0.689
33.24	IEGPY^{443}KPAA	22	loop	Glu410	0.756
55.53	GLETY^{328}PGVK	64	bend	Arg302 Arg302	0.091

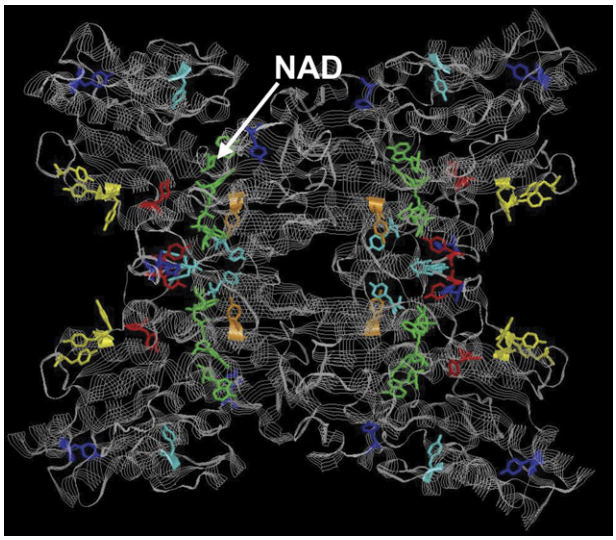

Fig. 6. Quaternary structure of the *Hordeum vulgare* tetrameric *S*-adenosyl-homocysteine hydrolase showing the localization of NAD (green colour) and Tyr residues coloured according to their rho value: rho = 1.1 orange, 6 <rho <7.3 red, 9 <rho <14 cyan, 14 <rho <19 yellow, rho >20 blue.

nitration in signalling pathways mediated by NO (Tedeschi *et al.*, 2007; Ischiropoulos, 2009). Until now, several proteomic studies have identified a relatively low number of nitrated proteins. Thus, a proteomic approach together with the use of a monoclonal antibody against nitrotyrosine has identified about 40 different proteins during inflammatory challenge in rat lung and liver. The proteins identified were involved in different functions such as oxidative stress, apoptosis, ATP production, and fatty acid metabolism (Aulak *et al.*, 2001). More recently, and also with the use of an antibody against nitrotyrosine, another proteomic identification of tyrosine nitration targets in the kidneys of hypertensive rats revealed the existence of 22 differentially nitrated proteins (Tyther *et al.*, 2007). However, only catalase and glyceraldehydes-3-phosphate dehydrogenase were coincident targets in the three rat organs analysed.

By contrast, in plants, much less information is available on the content of NO_2-Tyr and the identity of nitrated proteins. The simultaneous determination of NO_2-Tyr and Tyr in hypocotyl extracts was undertaken by a LC-MS/MS method previously used in animal tissues (Ishii *et al.*, 2006). In healthy mice liver, the reported Tyr concentration is 3.53 μmol mg^{-1} protein, this being approximately 6-fold lower in hypocotyls. However, the concentration of NO_2-Tyr is very similar being 0.19 pmol mg^{-1} protein in hypocotyls and 0.20 pmol mg^{-1} protein in mice liver (Ishii *et al.*, 2006) indicating that the putative functional behaviour of the NO_2-Try could be very similar in plants and animals. On the other hand, the NO_2-Tyr/Tyr ratio was 33.9 μmol mol^{-1} which is the same order of magnitude as the reported basal NO_2-Tyr/Tyr ratio in healthy rat kidney and mouse liver, which were 51.1 μmol mol^{-1} and 58.2 μmol mol^{-1}, respectively (Thierry *et al.*, 2002; Ishii *et al.*, 2006).

Furthermore, to our knowledge, there is still no protein identified with this post-translational modification. So far,

plant studies on this subject have focused on analysing whether or not the total content of nitrated proteins changed under certain stress conditions. For example, the leaves from salt-stressed olive trees registered an increase in the number of proteins of 44–60 kDa that underwent tyrosine nitration (Valderrama *et al.*, 2007). In nitrite reductase antisense tobacco leaves, the induction of several tyrosine-nitrated polypeptides with molecular masses between 10- and 50-kDa has been also reported (Morot-Gaudry-Talarmain *et al.*, 2002). Moreover, in tobacco BY-2 suspension cells treated with a fungal elicitor, the induction of tyrosine nitration in proteins with molecular masses in the range 20–50 kDa has been demonstrated (Saito *et al.*, 2006). Conversely, in tobacco transgenic plants with genetically increased cytokinin levels, the content of tyrosine nitrated proteins decreased (Wilhelmova *et al.*, 2006). More recently, in pea plants grown under several stress conditions (low temperature, high temperature, high light intensity, and continuous light) intensification in the proteins that undergo tyrosine nitration has been reported (Corpas *et al.*, 2008*b*). However, to our knowledge none of these proteins has yet been identified. All together, these data indicate that an increase in the number of proteins or an intensification of specific proteins that underwent tyrosine nitration could be considered a footprint of nitrosative stress, as has been proposed in animal cells (Ischiropoulos, 2003) and plants cells (Corpas *et al.*, 2007*b*, 2009; Valderrama *et al.*, 2007).

In this experimental design, sunflower plants grown under optimal conditions were used because this is a physiological process which eliminates the identification of artefacts that may arise when exposing cells or tissues to exogenous NO or nitrating agents. Thus, at least six immunoreactive bands in the molecular mass range of between 15 kDa and 68 kDa were found in this plant material. Considering that, in mammals, peroxynitrite ($ONOO^-$) has been shown to participate in the nitration of tyrosine residues of proteins (Ischiropoulos *et al.*, 1992; Radi, 2004; Naviliat *et al.*, 2005; van der Vliet, 2006; Peluffo and Radi, 2007), the presence and location of peroxynitrite by CLSM was also investigated. A close cellular location of NO_2-Tyr and $ONOO^-$ was found in hypocotyl sections, indicating that tyrosine nitration may also occur through peroxynitrite in sunflower hypocotyls.

A proteomic approach using a well-characterized antibody against NO_2-Tyr (Chaki, 2007; Valderrama *et al.*, 2007; Chaki *et al.*, 2009) was followed to gain knowledge on the nature of nitrated proteins (Butt and Lo, 2008). This allowed us to identify a total of 21 nitrated proteins, this number of proteins being consistent with previous proteomic identification analyses in animal systems (Aulak *et al.*, 2001; Tyther *et al.*, 2007). The proteins identified in different physiological processes included photosynthesis, the proteasome pathway, signalling, antioxidant, ATP, and carbohydrate and nitrogen metabolism. Among these proteins only a few were coincident with or similar to identified tyrosine-nitrated proteins in animals, such as glutathione reductase (Francescutti *et al.*, 1996), protein kinase (Balafanova *et al.*, 2002) or cytochrome P450 (Roberts *et al.*, 1998; Lin *et al.*, 2007), the rest of the proteins being new candidates.

On the other hand, *S*-nitrosylation is another relevant post-translation modification mediated by NO or NO-derived molecules. Thus, in *Arabidopsis* plants, several proteomic approaches have enabled the identification of candidates for this process, 63 proteins from cell cultures, 52 proteins from leaves (Lindermayr *et al.*, 2005), and 18 proteins during the hypersensitive response (Romero-Puertas *et al.*, 2008). A comparative analysis shows that among all these candidates, only the *S*-adenosyl-L-homocysteine hydrolase was also candidates for tyrosine nitration (present study). However, it is a good example of the connection between *S*-nitrosylation and tyrosine nitration. Thus, it has been described that peroxiredoxin II E from *Arabidopsis* possesses peroxynitrite reductase activity; however, the *S*-nitrosylation of this specific peroxiredoxin causes its inhibition and promotes an increase of tyrosine nitration (Romero-Puertas *et al.*, 2007).

To gain deeper insights into the biological significance of tyrosine nitration, *S*-adenosyl-L-homocysteine hydrolase (SAHH, EC 3.3.1.1) was selected to perform *in vitro* nitration assays using SIN-1 as the peroxynitrite donor because this protein seems to be regulated by RNS as well as by *S*-nitrosylation (Lindermayr *et al.*, 2005). SAHH activity is found in mammals, birds, plants, and yeast and is involved in the methylation cycle of genomic DNA catalysing the reversible breakdown of *S*-adenosyl-L-homocysteine to adenosine and homocysteine (Poulton and Butt, 1976; Mull *et al.*, 2006). The *in vitro* activity assay of this enzyme from sunflower hypocotyls in the presence of an increased concentration of $ONOO^-$ clearly demonstrated the inhibitory effect of this nitrating molecule on SAHH activity. Similar observations have been made in different studies on the nitration and inactivation by peroxynitrite of Mn-superoxide dismutase (Quijano *et al.*, 2001), glutathione reductase (Savvides *et al.* 2002), cytochrome P450 2B1 (Roberts *et al.*, 1998) or recombinant iron-superoxide dismutase from cowpea (Larrainzar *et al.*, 2008).

Nitration of tyrosine is a selective process. Usually proteins have approximately 3–4 mol% of Tyr but only one or two of these tyrosines become preferentially nitrated, this depending on several factors such as protein structure, nitration mechanism, and environment, where the protein is located (Bartesaghi *et al.*, 2007). For example, in chronic rejection of human renal allografts and in traumatic brain injury, it has also been reported that tyrosine nitration of manganese superoxide dismutase (Mn-SOD) increased, causing its further inactivation (MacMillan-Crow *et al.*, 1996; Bayır *et al.*, 2007). Later, it was confirmed by mass spectroscopic analysis that the peroxynitrite-inactivated Mn-SOD showed a single nitro group substituted onto a tyrosine residue (Tyr34) (Yamakura *et al.*, 1998).

For the identification of the Tyr residue/s potentially nitrated in SAHH, an *in silico* study was chosen. Since nitration of tyrosine plays a major role in protein

modulation, it must be a selective process with a well-defined target that is preserved throughout evolution. Thus, the evolutionary analysis of 500 sequences with *E*-value <*e*-102 indicates that Tyr207 is an extremely well-conserved residue with an outstanding rho of 1.1, suggesting an important role. The other Tyr candidates can be grouped into four categories: (i) Tyr434 and Tyr448 with rho values of between 6 and 7; (ii) Tyr82, Tyr450, and Tyr235 with rho values of around 10; (iii) Tyr397, Tyr402, and Tyr179 with rho values of around 15, and (iv) Tyr157, Tyr443, and Tyr328 with rho values higher than 20. However, a systematic analysis of nitrated proteins (Sacksteder *et al.*, 2006) in mouse brain revealed that almost 60% of the nitrated tyrosine sites are predicted to be located at loop sites, where the solvent accessible area is larger, with basic amino acids in the immediate vicinity within the primary sequence, suggesting the involvement of electrostatic attractions of nitrating anions, and in the proximity of a nearby negative charge that promotes the selective nitration under *in vitro* conditions (Souza *et al.*, 1999).

Regardless of any other consideration (i.e. evolutionary conservation and nearby-residue criterion), the nitration of Tyr82, Tyr450, Tyr157, Tyr235, or Tyr207 seems unlikely because their solvent-accessible surface area is 7, 8, 12, or 16 and 19 $Å^2$, respectively. Potential candidates with a large solvent-accessible surface areas are Tyr179 and Tyr328 but the fact that they are among the less preserved does not indicate a role in modulation. The same justification applies to rule out Tyr443, Tyr402, and Tyr397, which display smaller solvent-accessible surface areas and are predicted to be phosphorylation sites.

The two most probable targets for nitration are Tyr434 and Tyr448, the second and third best preserved with solvent-accessible surface areas of 70 $Å^2$ and 41 $Å^2$, respectively. However, although both are good candidates, Tyr434 fails the nearby-residue criterion, since neither the basic amino acids are in its immediate vicinity within the primary sequence nor are the acidic residues within 5 Å from the atom susceptible to nitration. The large phosphorylation score also supports Tyr434 as a phosphorylation target. Thus, Tyr448 is proposed as the target for the nitration because it is located in a loop and fulfils both the solvent-accessible surface area and the nearby-residue criterion with Lys444 and Arg449 within a nine-residue window and Asp237 within 5 Å from the atom susceptible to nitration. Moreover, its nitration is consistent with the observed inhibitory effect, since it is located at a position where its nitration would disrupt the NAD site.

In summary, the present study provides the concentration of nitrotyrosine and the first identification of proteins that undergo tyrosine nitration in plants under physiological conditions. In addition, it is demonstrated that the activity of SAHH, an enzyme involved in the methylation cycle of genomic DNA, is inhibited by peroxynitrite, a molecule which mediates tyrosine nitration, conserved Tyr448 being the most reliable candidate. Consequently, the physiological nitration of SAHH could represent a fraction of the pool of this protein *in vivo* and an additional mechanism of its regulation. Thus, if the peroxynitrite levels increase under certain cellular conditions the equilibrium can be broken, the consequence of which will be an increase in nitrated SAHH and inactivation of its activity. Considering that SAHH is a candidate for both *S*-nitrosylation (Lindermayr *et al.*, 2005) and tyrosine nitration (present study), this suggests that these two post-translational modifications may participate in the regulation of DNA methylation. At present, a comparative analysis has been started by proteomic approaches to identify whether some of these proteins or new ones are affected under stress conditions. This information will enable the identification of potential markers of nitrosative stress in plants.

Supplementary data

Supplementary data are available at *JXB* online.

Supplementary Fig. S1. Multiple-sequence alignments of *S*-adenosyl-L-homocysteine hydrolase (SAHH) from *Hordeum vulgare* (Q4LB20), *Triticum aestivum* (P32112), *Oryza sativa* (AAO72664), *Arabidopsis thaliana* (CAB09795), and *Petroselinum crispum* (Q01781).

Acknowledgements

MC acknowledges a PhD fellowship from the University of Jaén. JLP was partially supported by a grant from 'Programa de Retorno de Investigadores a Centros de Investigación y Universidades de Andalucía' (Junta de Andalucía, Spain) who is also indebted to Professor F Santoyo for his support. Sunflower seeds were kindly provided by María I Rodríguez (Koipesol Seeds SA). Confocal laser-scanning microscopy and LC/MS analyses were carried out at the Technical Services of the University of Jaén, and proteomic analyses were made at the Proteomic Service from the University of Córdoba. This work was supported by grants from the Ministry of Education and Science (BIO2006-14949-C02-01 and BIO2006-14949-C02-02) and Junta de Andalucía (group BIO286 and BIO192).

References

Abriata LA, Cassina A, Tórtora V, Marín M, Souza JM, Castro L, Vila AJ, Radi R. 2009. Nitration of solvent-exposed tyrosine-74 on cytochrome *c* triggers heme iron-methionine-80 bond disruption: nuclear magnetic resonance and optical spectroscopy studies. *Journal of Biological Chemistry* **284,** 17–26.

Altschul SF, Madden TL, Schäffer AA, Zhang J, Zhang Z, Miller W, Lipman DJ. 1997. Gapped BLAST and PSI-BLAST: a new generation of protein database search programs. *Nucleic Acids Research* **25,** 3389–3402.

Alvarez B, Radi R. 2003. Peroxynitrite reactivity with amino acids and proteins. *Amino Acids* **25,** 295–311.

Arnold K, Bordoli L, Kopp J, Schwede T. 2006. The SWISS-MODEL workspace: a web-based environment for protein structure homology modelling. *Bioinformatics* **22,** 195–201.

Aulak KS, Miyagi M, Yan L, West KA, Massillon D, Crabb JW, Stuehr DJ. 2001. Proteomic method identifies proteins nitrated *in vivo* during inflammatory challenge. *Proceedings of the National Academy of Sciences, USA* **98,** 12056–12061.

Balafanova Z, Bolli R, Zhang J, Zheng Y, Pass JM, Bhatnagar A, Tang XL, Wang O, Cardwell E, Ping P. 2002. Nitric oxide (NO) induces nitration of protein kinase Cepsilon (PKCepsilon), facilitating PKCepsilon translocation via enhanced PKCepsilon -RACK2 interactions: a novel mechanism of no-triggered activation of PKCepsilon. *Journal of Biological Chemistry* **277,** 15021–15027.

Bayir H, Kagan VE, Clark RS, Janesko-Feldman K, Rafikov R, Huang Z, Zhang X, Vagni V, Billiar TR, Kochanek PM. 2007. Neuronal NOS-mediated nitration and inactivation of manganese superoxide dismutase in brain after experimental and human brain injury. *Journal of Neurochemistry* **101,** 168–181.

Bartesaghi S, Ferrer-Sueta G, Peluffo G, Valez V, Zhang H, Kalyanaraman B, Radi R. 2007. Protein tyrosine nitration in hydrophilic and hydrophobic environments. *Amino Acids* **32,** 501–515.

Blom N, Gammeltoft S, Brunak S. 1999. Sequence- and structure-based prediction of eukaryotic protein phosphorylation sites. *Journal of Molecular Biology* **294,** 1351–1362.

Brunger AT, Adams PD, Clore GM, *et al*. 1998. Crystallography and NMR system (CNS). A new software system for macromolecular structure determination. *Acta Crystallographica* D **54,** 905–921.

Buchczyk DP, Briviba K, Hartl FU, Sies H. 2000. Responses to peroxynitrite in yeast: glyceraldehyde-3-phosphate dehydrogenase (GAPDH) as a sensitive intracellular target for nitration and enhancement of chaperone expression and ubiquitination. *Biological Chemistry* **381,** 121–126.

Butt YK, Lo SC. 2008. Detecting nitrated proteins by proteomic technologies. *Methods in Enzymology* **440,** 17–31.

Chaki M. 2007. Function of reactive nitrogen species in sunflower (*Helianthus annuus*) in response to abiotic and biotic stresses. PhD thesis, University of Jaén, Spain.

Chaki M, Fernández-Ocaña AM, Valderrama R, Carreras A, Esteban FJ, Luque F, Gómez-Rodríguez MV, Begara-Morales JC, Corpas FJ, Barroso JB. 2009. Involvement of reactive nitrogen and oxygen species (RNS and ROS) in sunflower-mildew interaction. *Plant and Cell Physiology* **50,** 265–279.

Chander PN, Gealekman O, Brodsky SV, Elitok S, Tojo A, Crabtree M, Gross SS, Goligorsky MS. 2004. Nephropathy in Zucker diabetic fat rat is associated with oxidative and nitrosative stress: prevention by chronic therapy with a peroxynitrite scavenger ebselen. *Journal of the American Society of Nephrology* **15,** 2391–2403.

Corpas FJ, Barroso JB, Carreras A, Valderama R, Palma JM, León AM, Sandalio LM, del Rio LA. 2006. Constitutive arginine-dependent nitric oxide synthase activity in different organs of pea seedlings during plant development. *Planta* **224,** 246–254.

Corpas FJ, Barroso JB, Sandallo LM, Distefano S, Palma JM, Lupiáñez JA, del Rio LA. 1998. A dehydrogenase-mediated recycling system of NADPH in plant peroxisomes. *Biochemical Journal* **330,** 777–784.

Corpas FJ, Carreras A, Valderrama R, Chaki M, Palma JM, del Río LA Barroso JB. 2007*a*. Reactive nitrogen species and nitrosative stress in plants. *Plant Stress* **1,** 37–41.

Corpas FJ, Chaki M, Fernández-Ocaña A, Valderrama R, Palma JM, Carreras A, Begara-Morales JC, Airaki M, del Río LA, Barroso JB. 2008*a*. Metabolism of reactive nitrogen species in pea plants under abiotic stress conditions. *Plant and Cell Physiology* **49,** 1711–1722.

Corpas FJ, Chaki M, Leterrier M, Barroso JB. 2009. Protein tyrosine nitration: a new challenge in plants. *Plant Signaling and Behavior* **4,** 1–4.

Corpas FJ, del Río LA, Barroso JB. 2007*b*. Need of biomarkers of nitrosative stress in plants. *Trends in Plant Science* **12,** 436–438.

Corpas FJ, del Río LA, Barroso JB. 2008*b*. Post-translational modifications mediated by reactive nitrogen species: nitrosative stress responses or components of signal transduction pathways? *Plant Signaling and Behaviour* **3,** 301–303.

Daiber A, Bachschmid M, Beckman JS, Munzel T, Ullrich V. 2004. The impact of metal catalysis on protein tyrosine nitration by peroxynitrite. *Biochemical and Biophysical Research Communications* **317,** 873–381.

Daiber A, Zou MH, Bachschmid M, Ullrich V. 2000. Ebselen as a peroxynitrite scavenger *in vitro* and *ex vivo*. *Biochemical Pharmacology* **59,** 153–160.

Eisenberg D, Lüthy R, Bowie JU. 1997. VERIFY3D: assessment of protein models with three-dimensional profiles. *Methods in Enzymology* **277,** 396–404.

Francescutti D, Baldwin J, Lee L, Mutus B. 1996. Peroxynitrite modification of glutathione reductase: modeling studies and kinetic evidence suggest the modification of tyrosines at the glutathione disulfide binding site. *Protein Engineering* **9,** 189–194.

Gow AJ, Farkouh CR, Munson DA, Posencheg MA, Ischiropoulos H. 2004. Biological significance of nitric oxide-mediated protein modifications. *American Journal of Physiology. Lung Cell Molecular Physiology* **287,** L262–L268.

Hensley K, Maidt ML, Yu Z, Sang H, Markesbery WR, Floyd RA. 1998. Electrochemical analysis of protein nitrotyrosine and dityrosine in the Alzheimer brain indicates region-specific accumulation. *Journal of Neuroscience* **18,** 8126–8132.

Ishii Y, Ogara A, Katsumata T, Umemura T, Nishikawa A, Iwasaki Y, Ito R, Saito K, Hirose M, Nakazawa H. 2006. Determination of nitrotyrosine and tyrosine by high-performance liquid chromatography with tandem mass spectrometry and immunohistochemical analysis in livers of mice administered acetaminophen. *Journal of Pharmaceutical and Biomedical Analysis* **41,** 1325–1331.

Ischiropoulos H. 2003. Biological selectivity and functional aspects of protein tyrosine nitration. *Biochemical and Biophysical* Research *Communications* **305,** 776–783.

Ischiropoulos H. 2009. Protein tyrosine nitration: an update. *Archives of Biochemistry and Biophysics* **484,** 117–121.

Ischiropoulos H, Zhu L, Chen J, Tsai M, Martin JC, Smith CD, Beckman JS. 1992. Peroxynitrite-mediated tyrosine nitration catalyzed by superoxide dismutase. *Archives of Biochemistry and Biophysics* **298,** 431–437.

Ji Y, Neverova I, Van Eyk JE, Bennett BM. 2006. Nitration of tyrosine 92 mediates the activation of rat microsomal glutathione *S*-transferase by peroxynitrite. *Journal of Biological Chemistry* **281,** 1986–1991.

Kloor D, Yao K, Delabar Y, Osswald H. 2000. Simple and sensitive binding assay for measurement of adenosine using reduced *S*-adenosylhomocysteine hydrolase. *Clinical Chemistry* **46,** 537–542.

Kabsch W, Sander C. 1983. Dictionary of protein secondary structure: pattern recognition of hydrogen bonded and geometrical features. *Biopolymers* **22,** 2577–2637.

Laemmli UK. 1970. Cleavage of structural proteins during the assembly of the head of bacteriophage T4. *Nature* **227,** 680–685.

Larrainzar E, Urarte E, Auzmendi I, Ariz I, Arrese-Igor C, González EM, Moran JF. 2008. Use of recombinant iron-superoxide dismutase as a marker of nitrative stress. *Methods in Enzymology* **37,** 605–618.

Laskowski RA, MacArthur MW, Moss DS, Thornton JM. 1993. PROCHECK: a program to check the stereochemical quality of protein structures. *Journal of Applied Crystallography* **26,** 283–291.

Lin HL, Myshkin E, Waskell L, Hollenberg PF. 2007. Peroxynitrite inactivation of human cytochrome P450s 2B6 and 2E1: heme modification and site-specific nitrotyrosine formation. *Chemical Research in Toxicology* **20,** 1612–1622.

Lindermayr C, Saalbach G, Durner J. 2005. Proteomic identification of *S*-nitrosylated proteins in Arabidopsis. *Plant Physiology* **137,** 921–930.

MacMillan-Crow LA, Crow JP, Kerby JD, Beckman JS, Thompson JA. 1996. Nitration and inactivation of manganese superoxide dismutase in chronic rejection of human renal allografts. *Proceedings of the National Academy of Sciences, USA* **93,** 11853–11858.

McRee DE. 1993. *Practical protein crystallography*. San Diego: Academic Press.

Melo F, Feytmans E. 1998. Assesing protein structures with a non-local atomic interaction energy. *Journal of Molecular Biology* **227,** 1141–1152.

Mihalek I, Res I, Lichtarge O. 2004. A family of evolution-entropy hybrid methods for ranking protein residues by importance. *Journal of Molecular Biology* **336,** 1265–1282.

Morot-Gaudry-Talarmain Y, Rockel P, Moureaux T, Quillere I, Leydecker MT, Kaiser WM, Morot-Gaudry JF. 2002. Nitrite accumulation and nitric oxide emission in relation to cellular signaling in nitrite reductase antisense tobacco. *Planta* **215,** 708–715.

Mull L, Ebbs ML, Bender J. 2006. A histone methylation-dependent DNA methylation pathway is uniquely impaired by deficiency in Arabidopsis *S*-adenosylhomocysteine hydrolase. *Genetics* **174,** 1161–1171.

Naviliat M, Gualco G, Cayota A, Radi R. 2005. Protein 3-nitrotyrosine formation during *Trypanosoma cruzi* infection in mice. *Brazilian Journal of Medical and Biological Research* **38,** 1825–1834.

Peluffo G, Radi R. 2007. Biochemistry of protein tyrosine nitration in cardiovascular pathology. *Cardiovascular Research* **75,** 291–302.

Perkins DN, Pappin DJ, Creasy DM, Cottrell JS. 1999. Probability-based protein identification by searching sequence databases using mass spectrometry data. *Electrophoresis* **20,** 3551–3567.

Poulton JE, Butt VS. 1976. Purification and properties of *S*-adenosyl-L-homocysteine hydrolase from leaves of spinach beet. *Archives of Biochemistry and Biophysics* **172,** 135–142.

Quijano C, Hernandez-Saavedra D, Castro L, McCord JM, Freeman BA, Radi R. 2001. Reaction of peroxynitrite with Mn-superoxide dismutase. Role of the metal center in decomposition kinetics and nitration. *Journal of Biological Chemistry* **276,** 11631–11638.

Radi R. 2004. Nitric oxide, oxidants, and protein tyrosine nitration. *Proceedings of the National Academy of Sciences, USA* **101,** 4003–4008.

Roberts ES, Lin H, Crowley JR, Vuletich JL, Osawa Y, Hollenberg PF. 1998. Peroxynitrite-mediated nitration of tyrosine and inactivation of the catalytic activity of cytochrome P450 2B1. *Chemical Research in Toxicology* **11,** 1067–1074.

Romero-Puertas MC, Laxa M, Mattè A, Zaninotto F, Finkemeier I, Jones AME, Perazzolli M, Vandelle E, Dietz K-J, Delledonne M. 2007. *S*-nitrosylation of peroxiredoxin II E promotes peroxynitrite-mediated tyrosine nitration. *The Plant Cell* **19,** 4120–4130.

Romero-Puertas MC, Campostrini N, Mattè A, Righetti PG, Perazzolli M, Zolla L, Roepstorff P, Delledonne M. 2008. Proteomic analysis of *S*-nitrosylated proteins in *Arabidopsis thaliana* undergoing hypersensitive response. *Proteomics* **8,** 1459–1469.

Rubbo H, Radi R. 2008. Protein and lipid nitration: role in redox signaling and injury. *Biochimica et Biophysica Acta* **1780,** 1318–1324.

Sacksteder CA, Qian WJ, Knyushko TV, *et al*. 2006. Endogenous nitrated proteins in mouse brain: links to nerugodegenerative disease. *Biochemisty* **45,** 8009–8022.

Saito S, Yamamoto-Katou A, Yoshioka H, Doke N, Kawakita K. 2006. Peroxynitrite generation and tyrosine nitration in defense responses in tobacco BY-2 cells. *Plant and Cell Physiology* **47,** 689–697.

Savvides SN, Scheiwein M, Bohme CC, Arteel GE, Karplus PA, Becker K, Schirmer RH. 2002. Crystal structure of the antioxidant enzyme glutathione reductase inactivated by peroxynitrite. *Journal of Molecular Biology* **277,** 2779–2784.

Schopfer FJ, Baker PR, Freeman BA. 2003. NO-dependent protein nitration: a cell signaling event or an oxidative inflammatory response? *Trends in Biochemical Sciences* **28,** 646–654.

Souza JM, Daikhin E, Yudkoff M, Raman CS, Ischiropoulos H. 1999. Factors determining the selectivity of protein tyrosine nitration. *Archives of Biochemistry and Biophysics* **371,** 169–178.

Souza JM, Peluffo G, Radi R. 2008. Protein tyrosine nitration: functional alteration or just a biomarker? *Free Radical Biology and Medicine* **45,** 357–366.

Tanaka N, Nakanishi M, Kusakabe Y, Shiraiwa K, Yabe S, Ysutomo I, Kitade Y, Nakamura KT. 2004. Crystal structure of *S*-adenosyl-L-homocysteine hydrolase from the human malaria parasite

Plasmodium falciparum. *Journal of Molecular Biology* **343,** 1007–1017.

Tedeschi G, Cappelletti G, Nonnis S, Taverna F, Negri A, Ronchi C, Ronchi S. 2007. Tyrosine nitration is a novel post-translational modification occurring on the neural intermediate filament protein peripherin. *Neurochemical Research* **32,** 433–441.

Thierry D, Janique R, Jacques V, Richard HS. 2002. Artifactual nitration controlled measurement of protein-bound 3-nitro-L-tyrosine in biological fluids and tissues by isotope dilution liquid chromatography electrospray ionization tandem mass spectrometry. *Chemical Research in Toxicology* **15,** 1209–1217.

Thiede B, Höhenwarter W, Krah A, Mattow J, Schmid M, Schmidt F, Jungblut PR. 2005. Peptide mass fingerprinting. *Methods* **35,** 237–247.

Tsikas D, Mitschke A, Suchy MT, Gutzki FM, Stichtenoth DO. 2005. Determination of 3-nitrotyrosine in human urine at the basal state by gas chromatography-tandem mass spectrometry and evaluation of the excretion after oral intake. *Journal of Chromatography B Analytical Technologies in the Biomedical and Life Sciences* **827,** 146–156.

Turko IV, Murad F. 2002. Protein nitration in vascular diseases. *Pharmacological Research* **54,** 619–634.

Tyther R, Ahmeda A, Johns E, Sheehan D. 2007. Proteomic identification of tyrosine nitration targets in kidney of spontaneously hypertensive rats. *Proteomics* **7,** 4555–4564.

Uttenthal LO, Alonso D, Fernádez AP, *et al*. 1998. Neuronal and inducible nitric oxide synthase and nitrotyrosine immunoreactivities in the cerebral cortex of the aging rat. *Microscopy Research and Technique* **43,** 75–88.

Valderrama R, Corpas FJ, Carreras A, Gómez-Rodríguez MV, Chaki M, Pedrajas JR, Fernández-Ocaña A, Del Río LA, Barroso JB. 2006. The dehydrogenase-mediated recycling of NADPH is a key antioxidant system against salt-induced oxidative stress in olive plants. *Plant, Cell and Environment* **29,** 1449–1459.

Valderrama R, Corpas FJ, Carreras A, Fernández-Ocaña A, Chaki M, Luque F, Gómez-Rodríguez MV, Colmenero-Varea P, del Río LA, Barroso JB. 2007. Nitrosative stress in plants. *FEBS Letters* **581,** 453–461.

van der Vliet A. 2006. Tyrosine nitration: who did it, and how do we prove it? A commentary on 'pH dependent nitration of para-hydroxyphenylacetic acid in the stomach'. *Free Radical Biology and Medicine* **41,** 869–871.

Wilhelmova N, Fuksova H, Srbova M, Mikova D, Mytinova Z, Prochazkova D, Vytasek R, Wilhelm J. 2006. The effect of plant cytokinin hormones on the production of ethylene, nitric oxide, and protein nitrotyrosine in ageing tobacco leaves. *Biofactors* **27,** 203–211.

Wong PS, van der Vliet A. 2002. Quantitation and localization of tyrosine nitration in proteins. *Methods in Enzymology* **359,** 399–410.

Yamakura F, Taka H, Fujimura T, Murayama K. 1998. Inactivation of human manganese-superoxide dismutase by peroxynitrite is caused by exclusive nitration of tyrosine 34 to 3-nitrotyrosine. *Journal of Molecular Biology* **273,** 14085–14089.